Proceedings of CHT-17
ICHMT International Symposium on Advances in Computational Heat Transfer

May 28-June 1, 2017, Napoli, Italy

CHT-17-155

THERMODIFFUSION EFFECTS ON LDL DEPOSITION IN A CURVED ARTERY

Marcello Iasiello[*], Kambiz Vafai[**], Assunta Andreozzi[*,§], Nicola Bianco[*]
[*]Dipartimento di Ingegneria Industriale, Università degli Studi di Napoli Federico II, Napoli, Italy
[**]Department of Mechanical Engineering, University of California, Riverside, CA 92521, USA
[§] Corresponding author. Fax: +39 081 239 0364; Email: assunta.andreozzi@unina.it

ABSTRACT In the atherosclerotic plaque formation process, LDL deposition through the wall plays a primary role. The multi-layer model, in which the heterogeneity of the arterial wall is taken into account by incorporating different layers, is the most robust and comprehensive approach. Recent research work has established that hyperthermia affects LDL profiles across the arterial wall mainly due to the Ludwig-Soret effect. In this work, hyperthermia effects on LDL deposition in a curved artery have been analyzed. Well-established thermophysical properties for each layer are taken from the literature. Mass, momentum, LDL concentration and energy equations are numerically solved for both lumen and the arterial wall with the latter modelled by volume-averaged porous media equations. LDL deposition and hyperthermia within the wall are coupled by a term in the concentration equation that takes into account the Ludwig-Soret effect. To validate our model comparisons with numerical and analytical solutions for isothermal straight and curved arteries are presented. Results show that radius of curvature of the artery has a relatively minor affect on LDL deposition with or without the presence of hyperthermia.

NOMENCLATURE

Latin symbols

c	Concentration (mol/m^3)
D	Diffusivity (m^2/s)
k	Reaction rate (1/s)
k_T	Thermodiffusion coefficient
K	Permeability (m^2)
L	Length (m)
M	Molecular weight (kg/mol)
p	Pressure (Pa)
r	Lumen radius (m)
R	Curvature radius (m)
T	Temperature (K)
$\mathbf{u}$	Velocity (m/s)
u,v	Velocity components (m/s)
x,y	Cartesian coordinates (m)
z	Lumen/endothelium interface coordinate (m)
WSS	Wall Shear Stress (Pa)

Greek symbols

α	Thermal diffusivity(m^2/s)
μ	Dynamic viscosity (kg/m·s)
ρ	Density (kg/m^3)
σ	Reflection coefficient

Other

$\langle\ \rangle$	Average

Subscript

0	Reference value
max	Maximum value

INTRODUCTION

Low-Density Lipoprotein (LDL) plays a crucial role in atherosclerosis genesis. The atherosclerotic plaque growth is strongly influenced by LDL infiltration through the arterial wall, since it tends to recall monocytes from the lumen, to form foam cells that attract smooth muscle cells from the exterior parts of the wall, causing the plaque to restrict the free blood flow passage section. This restriction can cause various diseases such as a heart attack or ischemia. As such predicting LDL deposition through an arterial wall is very important in order to clearly understand the atherosclerotic plaque growth process.

The scientific community is paying much attention into analyzing LDL deposition phenomena. Since experiments are difficult to carry out, numerical and analytical analyses are very helpful. Three main models have been employed in the past [*e.g.*, Prosi *et al.* 2005]. The first is the wall-free model, in which the arterial wall is replaced with a boundary condition [*e.g.*, Wada and Karino 2000]. The second is the single layer model, where the wall is modeled as a homogeneous tissue [*e.g.*, Stangeby and Ethier 2002]. The latter technique which is substantially more accurate, considers LDL deposition in various layers which is far more realistic. For example, predicting deposition in the tunica intima is very important, since it is the layer in which the plaque grows. Therefore modeling the wall as a heterogeneous layer (multi-layer model [*e.g.*, Yang and Vafai 2006 and Ai and Vafai 2006]) is far more accurate. Multi-layer models are now widely used.

Axi-symmetric straight medium arteries were analyzed both numerically [*e.g.*, Yang and Vafai 2006 and Ai and Vafai 2006] and analytically [*e.g.*, Khakpour and Vafai 2008, Wang and Vafai 2015 and Iasiello *et al.* 2016a]. The hypertension effects were analyzed by Yang and Vafai [2006], concluding that hypertension, *i.e.* increasing of transmural pressure between the two extremities of the arterial wall, increases LDL concentration within the artery. Effects of plaque thickness were analyzed for stenosed arteries [e.g., Ai and Vafai, 2006, Olgac *et al.* 2008, Nematollahi *et al.* 2012]. Chung and Vafai [2013] analyzed the plaque evolution by considering the thermophysical properties changes. The cholesterol lipid accumulation was modeled by using the fiber matrix model. Iasiello *et al.* [2015] analyzed thermodiffusion effects in a stenosed artery, concluding that these generally enhance LDL deposition. Carotid bifurcation was analyzed by Kenjeres and de Loor [2014], based on simulations for a multi-layered carotid bifurcation obtained with tomographic scans. The aorta-iliac bifurcation has been analyzed by Iasiello *et al.* [2016b] with a two-dimensional geometrical model. In the latter work, the authors conclude that flow recirculation might occur for high Reynolds number, causing a local enhancement in terms of LDL deposition at the lumen/endothelium interface.

Among various geometries, little attention has been paid to curved arteries. Indeed, the flow field, and consequently the LDL deposition, is affected by the radius of curvature of the artery. Wang and Vafai [2015] derived an analytical solution for a curved artery. They took into account the secondary flow which exists in the lumen region, incorporating and analyzing both the core and the boundary layer regions. Detailed analytical expressions were derived for the concentration distributions within the arterial wall. They concluded that, at equal lumen radii, higher curvature causes lower concentration on the exterior part of the curved artery.

Hyperthermia is a technique widely used in medicine for treating various diseases, such as thermal ablation of liver tumors or arrhythmias. It can be also used for laser angioplasty [*e.g.* Köster *et al.* 2002], that is a technique in which atherosclerotic plaques can be removed by applying a certain thermal dose by using a catheter equipped with a laser. Thermal effects on LDL transport occur via Ludwig-Soret effect (also known as thermodiffusion effect), with which solute particles move if a certain temperature difference is applied [*e.g.,* Platten 2006]. A comprehensive analysis of thermal effects on LDL transport in a straight artery was carried out by Chung and Vafai [2014], considering both thermal expansion and Ludwig-Soret effects. They concluded that LDL transport is generally enhanced when a certain thermal dose is applied to the wall. Thermodiffusion effects were analyzed for a stenosed artery by Iasiello *et al.* [2015], while an analytical solution for LDL transport under hypertension and hyperthermia conditions was derived by Iasiello *et al.* [2016a]).

In the present study, thermodiffusion effects on LDL transport in a curved artery are analyzed. After validating the model, wall shear stresses and LDL transport are computed for different curvatures. The target of the present study is to analyze the curvature effect on thermodiffusion and LDL deposition.

MATHEMATICAL MODEL

Geometry An arterial wall is made up of four layers. The first is the endothelium that is a membrane in direct contact with the lumen. This layer is made up of cells stretched along the flow direction, and it has a primary role in the filtration of the blood flow and its solutes across the wall. Its thermophysical properties depend on its integrity [*e.g.*, Chung and Vafai 2012]. The second layer is the tunica intima, made up of connective tissue. This is the layer in which the atherosclerotic plaque tends to grow, so predicting LDL in this layer is of primary importance. The third layer is the Internal Elastic Lamina (IEL) which is a membrane that separates the tunica intima from the tunica media which is the fourth layer. The tunica media is made up of connective tissue and Smooth Muscle Cells (SMC). After the tunica media, there is the tunica adventitia which is modeled with a boundary condition between the tunica media and adventitia. A sensitivity analysis on the appropriate boundary condition at the media/adventitia interface was carried out by Yang and Vafai [2006]. A sketch of an artery is depicted in Fig. 1.

In order to analyze the curvature effects, a straight artery is designed with different curvature ratios r/R, where r is the lumen radius and R the curvature radius of the artery. It is important to observe that if $R\rightarrow\infty$ then $r/R \rightarrow 0$, and the artery becomes a straight artery again. Curvature effects on the geometry are depicted in Fig. 1.

Governing equations In order to solve velocity, temperature and concentration fields, governing equations for mass, momentum, energy and concentration are employed. For the free flow (lumen), Navier-Stokes equations are employed, while for the wall layers equations are written with references to the porous media theory. The following assumptions are invoked:

- Flow is steady, incompressible and Newtonian (μ = 0.72 mPa·s) [*e.g.*, Iasiello *et al.* 2016b],
- Buoyancy effects are negligible,
- Thermophysical properties are uniform across the computational domain,
- Osmosis effects on the flow field can be neglected [e.g., Yang and Vafai 2006],
- Dufour effect is negligible [*e.g.*, Chung and Vafai 2014],
- Local Thermal Equilibirum (LTE) exists between the two phases [*e.g.*, Amiri and Vafai 1994 and Alazmi and Vafai 2001].

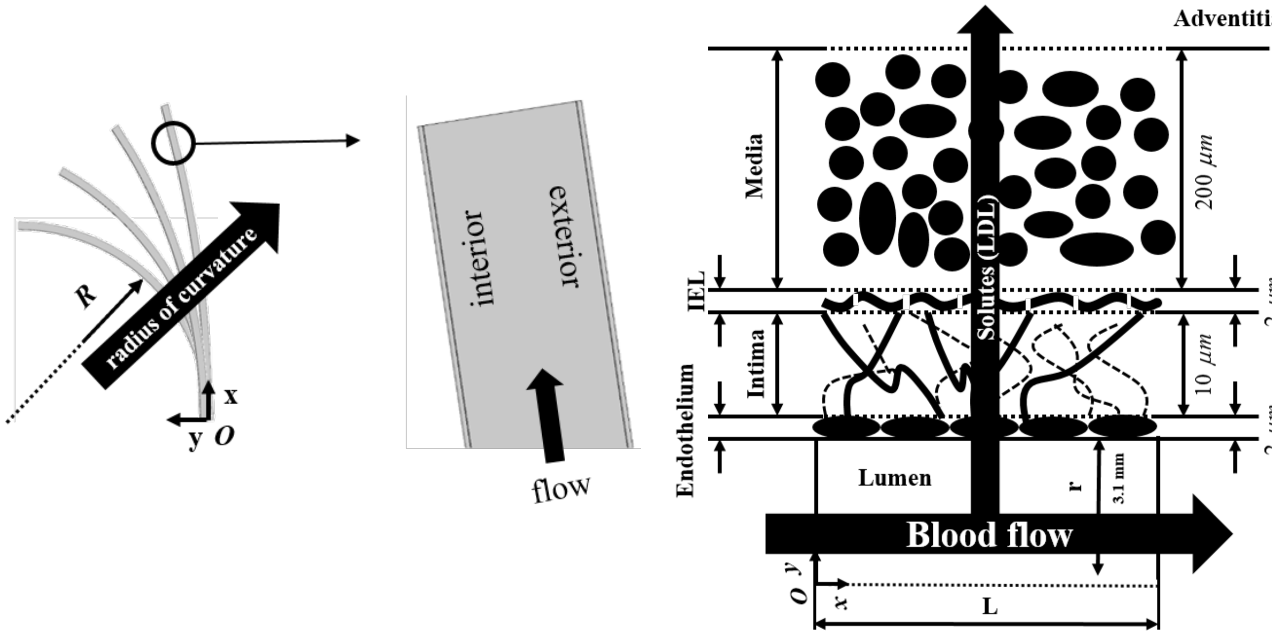

Figure 1: Curvature and arterial wall

Governing equations for the lumen region are:

$$\nabla \cdot \mathbf{u} = 0 \tag{1}$$

$$\rho \mathbf{u} \cdot \nabla \mathbf{u} = -\nabla p + \mu \nabla^2 \mathbf{u} \tag{2}$$

$$\mathbf{u} \cdot \nabla c = D \nabla^2 c \tag{3}$$

where **u** is the velocity vector, ρ density, p pressure, μ viscosity, c LDL concentration and D is the diffusivity. The energy equation is replaced with a uniform temperature boundary condition at the lumen/endothelium interface. Governing equations for the porous layers can be written as (Yang and Vafai 2006; Chung and Vafai 2014):

$$\nabla \cdot \langle \mathbf{u} \rangle = 0 \tag{4}$$

$$\nabla \langle p \rangle = \mu \nabla^2 \langle \mathbf{u} \rangle - \frac{\mu}{K} \langle \mathbf{u} \rangle \tag{5}$$

$$(1-\sigma) \langle \mathbf{u} \rangle \cdot \nabla \langle c \rangle = D \nabla^2 \langle c \rangle + \frac{k_T \rho}{M} \frac{D}{\langle T \rangle} \nabla^2 \langle T \rangle - k \langle c \rangle \tag{6}$$

$$\langle \mathbf{u} \rangle \cdot \nabla \langle T \rangle = \alpha \nabla^2 \langle T \rangle \tag{7}$$

where K is the permeability, σ the reflection coefficient, k_T the thermodiffusion coefficient, M the molecular weight, T the temperature, k the reaction rate and α is the thermal diffusivity. In the concentration equation, the term $k\langle c \rangle$ represents a first-order reaction that occurs in the media layer due to the solute uptake by the SMC. In order to close governing equations, values for density ρ, viscosity μ, diffusivity D, permeability K, and first-order reaction term k are required. These values are the same as those used in Yang and Vafai [2006] and Wang and Vafai [2015], which are presented in

Table 1. The value of the thermal diffusivity α is $1.42 \cdot 10^{-7}$ m^2/s [*e.g.*, Duck 1990 and Kolios *et al.* 1995].

Table 1
Thermophysical properties herein employed

Layer	Thickness (mm)	K (m^2)	D (m^2/s)	σ	k (1/s)
Lumen	6.2		$2.87 \cdot 10^{-11}$		
Endothelium	$2 \cdot 10^{-3}$	$4.32 \cdot 10^{-21}$	$6.00 \cdot 10^{-17}$	0.9979	
Intima	$10 \cdot 10^{-3}$	$2.00 \cdot 10^{-16}$	$5.40 \cdot 10^{-12}$	0.8272	
IEL	$2 \cdot 10^{-3}$	$4.39 \cdot 10^{-19}$	$3.18 \cdot 10^{-15}$	0.9827	
Media	$200 \cdot 10^{-3}$	$2.00 \cdot 10^{-18}$	$5.00 \cdot 10^{-14}$	0.8836	$3.20 \cdot 10^{-4}$

Boundary conditions For the lumen, at the inlet section of the artery, a parabolic fully developed velocity profile is employed:

$$u = u_{\max}\left[1-\left(y/r\right)\right]^2 \tag{8}$$

where u_{max} is the maximum velocity, y the transversal rectangular coordinate and r the lumen radius. The maximum value of the velocity is set equal to 0.338 m/s [*e.g.*, Karner *et al.* 2001]. The concentration is taken as uniform, with a value of $c_0 = 28.6 \cdot 10^{-3}$ mol/m^3 [*e .g.*, Katz 1985]. At the outlet section, a uniform pressure value of 100 mmHg is employed, with no shear stress, while an outflow condition for the concentration equation is employed. At the lumen/endothelium interfaces, continuity equations for the LDL are invoked.

For the porous layers, at the inlet/outlet section, zero flux conditions are used, in order to represent the periodicity of an artery. The periodicity conditions have been analyzed in detail in earlier works (Yang and Vafai 2006; Ai and Vafai 2006). For the energy equation, a uniform temperature boundary condition is applied at the lumen/endothelium interface, while again zero flux boundary conditions are employed in order to represent the periodicity of an artery (Yang and Vafai 2006; Ai and Vafai 2006). At the wall interfaces, continuity conditions for the heat flux and LDL concentrations are employed. At the media/adventitia interface, a 30 mmHg pressure boundary condition is employed, in order to achieve a 70 mmHg transmural pressure driving force. Outflow and uniform temperature boundary conditions are employed for the concentration and for the energy equations, respectively. From this point on, the symbol of volume-averaging $\langle \ \rangle$ will be dropped for convenience.

Numerical modeling The governing equations subject to the stated boundary conditions are solved with a finite element scheme by employing the commercial code COMSOL Multiphysics. For high r/R, a quadrilateral mesh (about 600,000 elements) is used, while for low r/R a triangular boundary layer mesh (about 3,500,000 elements) is employed since an increase in terms of the curvature makes triangular meshes more convenient. Grid convergence has been checked by verifying that the deviation for concentration profiles in the middle longitudinal section of an artery becomes negligible, i.e. less than 10^{-3}. A convergence criterion of 10^{-6} for the governing equations is employed.

RESULTS

Comparisons with numerical results from Yang and Vafai [2006], Figs. 2(a) and 2(b), and with analytical solutions from Wang and Vafai [2015], Fig.2 (a), and Iasiello *et al.* [2016a], Fig. 2(c), are reported in Fig. 2. Comparisons are reported for dimensionless concentration c/c_0 along the

lumen/endothelium interface, filtration velocity along the lumen/endothelium interface and dimensionless concentration along the wall thickness. A good agreement is exhibited in all the cases, with a deviation always less than about 0.5%. For the curved artery, it is noted that we are referencing the exterior part of the artery, in which the concentration tends to decrease.
Wall Shear Stresses (WSS) for the exterior part and for various curvature ratios are presented in Fig. 3. It is shown that they increase slightly with higher curvature ratios. A comparison between the interior and the exterior part of an artery is shown in Fig. 3b. It is shown that in the exterior part the WSS increases, while it decreases in the interior part. However, such differences are quite small.
The curvature effect is represented in Fig. 4 for the exterior part. It is shown that the lower the curvature ratio *r/R*, the higher is the concentration. This occurs because velocity fields are affected by the curvature of the artery, at equal inlet mass flow rates. This is consistent with the results from Wang and Vafai [2015], in which concentration is slightly lower than a straight artery since the exterior part of the lumen is considered. Curvature effect between the interior and the exterior part of the artery is presented in Fig. 4b, for *r/R* = 0.004. It is shown that the solute tends to accumulate more at the interior part of the artery than at the exterior segment.

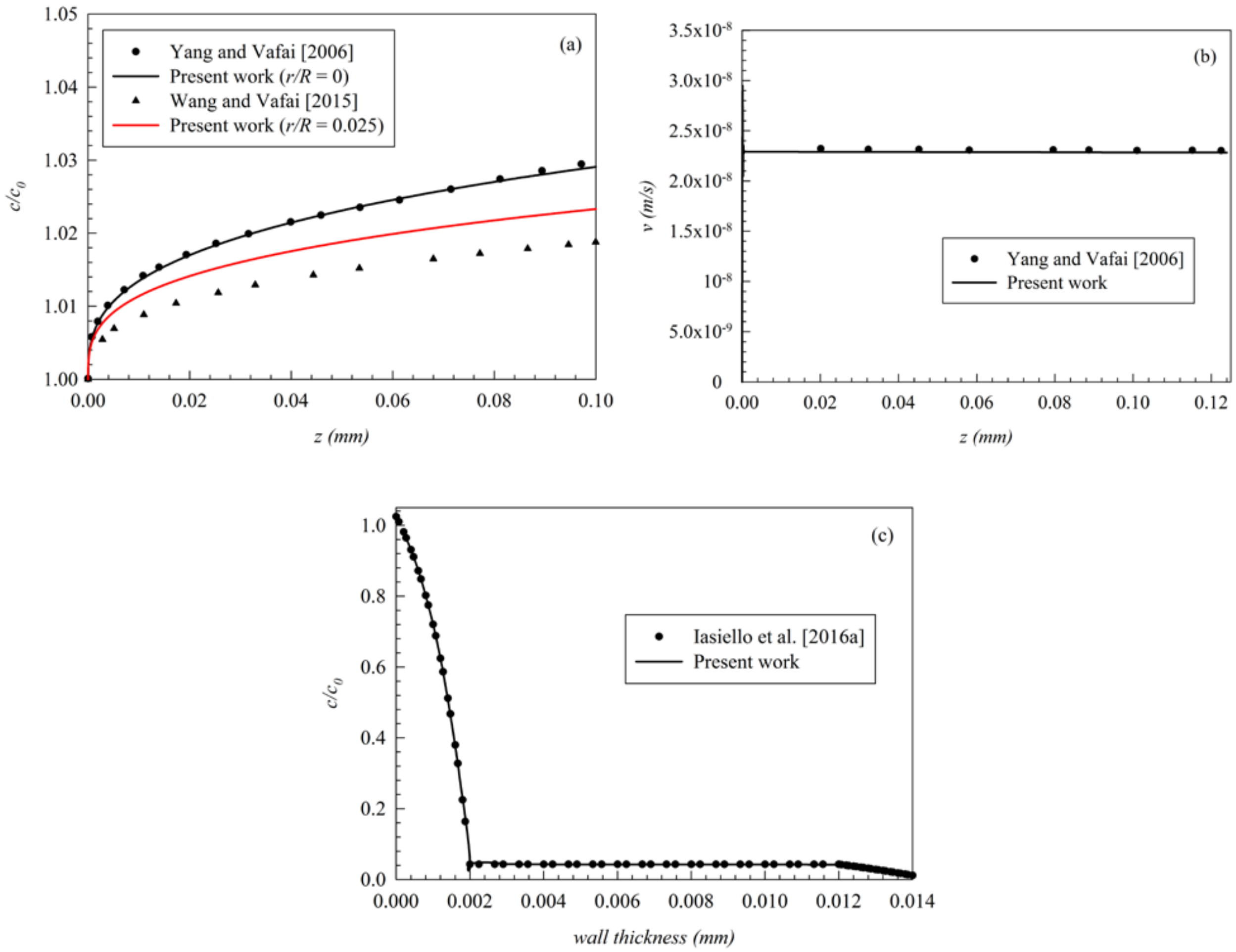

Fig. 2: Comparisons with results from literature

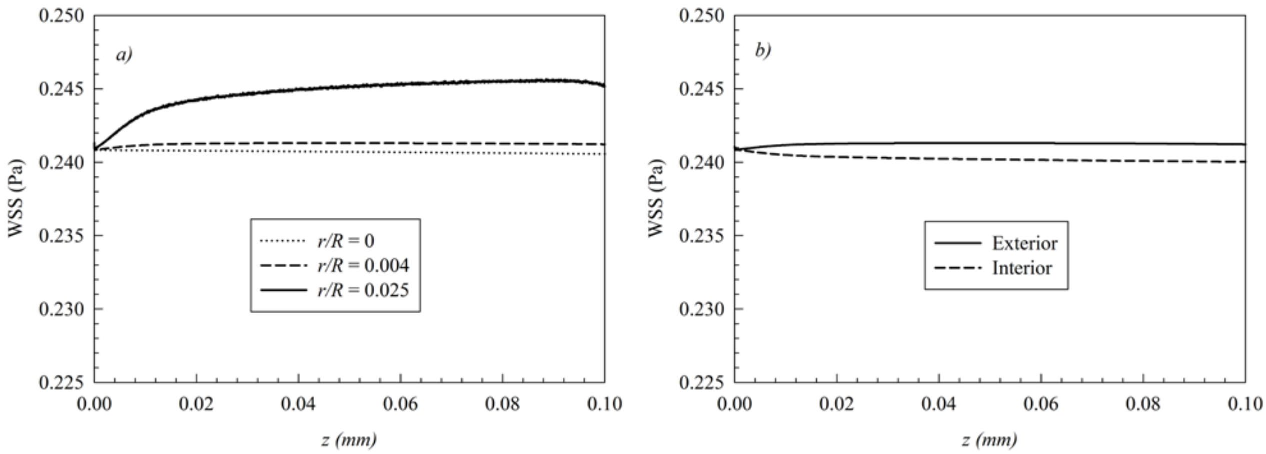

Fig. 3: *a)* curvature effect and *b)* location effect on WSS along the axial coordinate for $r/R = 0.025$

For the study of hyperthermia effects, properties from Chung and Vafai [2012] are employed. Temperature fields, contours and profiles for a curved artery are presented in Figs. 5 and 6, either for a heat flux applied from the exterior part of the artery (external heating) or from the interior (internal heating). It is shown that the temperature profile is practically linear, due to the very low Peclet number, with which the problem becomes almost only conductive [*e.g.*, Iasiello *et al.* 2015]. Indeed, isothermal contours follow the curvature of the artery.

The concentration fields for the external and internal heating, for $\Delta T = 20$ °C and $k_T = 0.0025$ and 0.005 are presented in Fig. 7.

It is shown that the curvature doesn't have much effect on LDL deposition. This is because the heat flux has always a normal direction with respect to the walls, so both gradients and temperature levels are not affected by the curvature (Eq. 6) and only slight differences are caused at different axial coordinates of the profiles. Indeed, the concentration profile along the arterial wall is affected by the concentration polarization effect, since the concentration at the lumen/endothelium interface changes (Yang and Vafai [2006]).

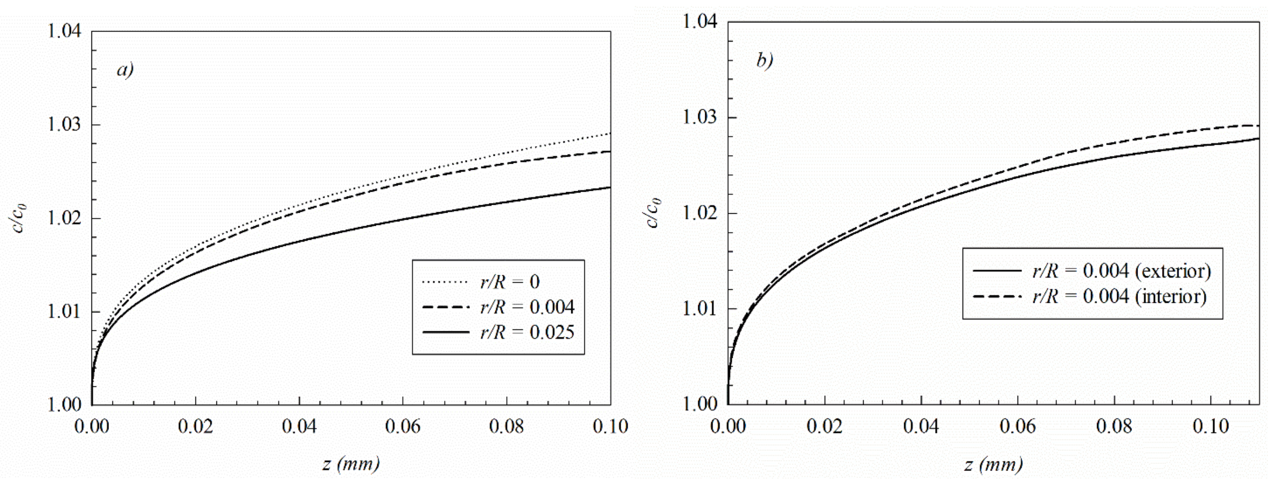

Fig. 4: *a)* curvature effect and *b)* location effect on LDL concentration along the axial coordinate

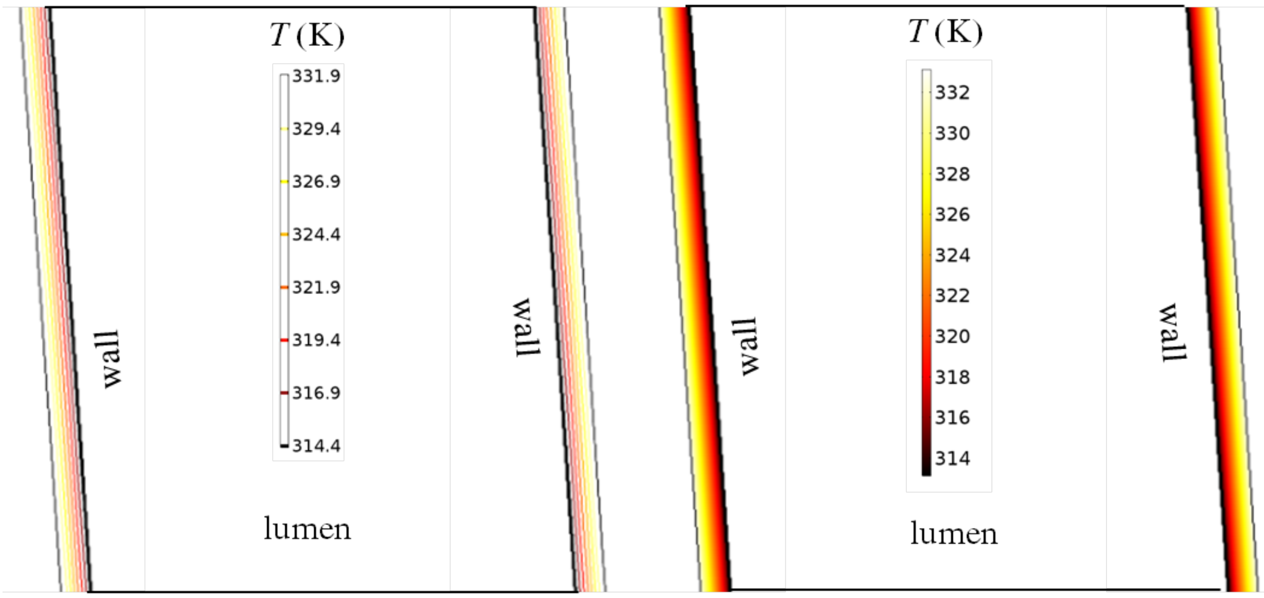

Fig. 5: Temperature contours and fields under external heating

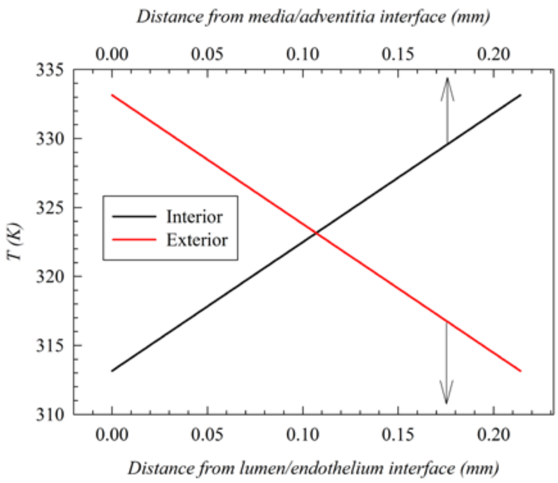

Fig. 6: Temperature profiles at different interface locations for internal and external heating

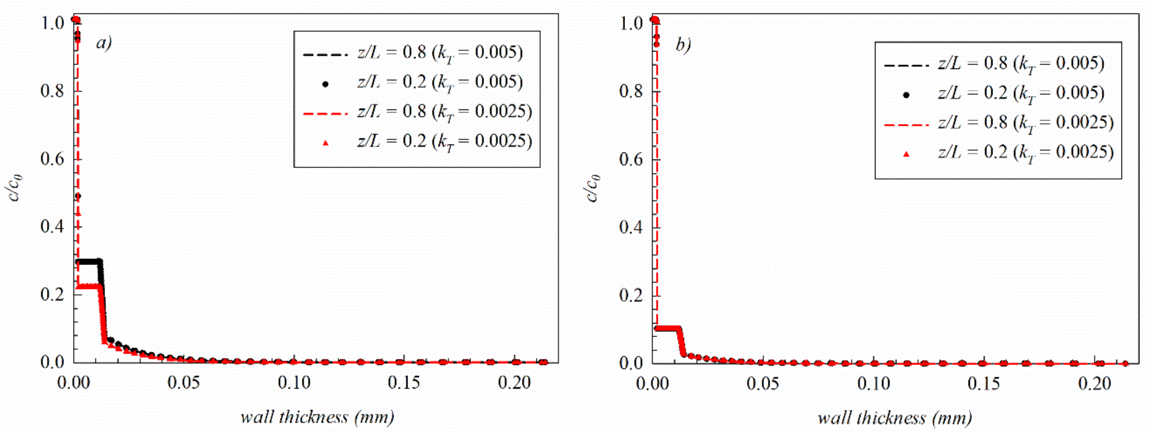

Fig. 7: Concentration profiles for a) external heating and b) internal heating

CONCLUSIONS

Thermodiffusion effects on LDL transport in a curved artery were analyzed. The geometry of the artery was modeled as a longitudinal section of an artery and a multi-layer model of the arterial wall was employed. Numerical results were obtained by means of the commercial code COMSOL Multiphysics. The numerical model was validated by comparing the present results with those of prior works in the literature. The comparison displayed a good agreement between the current results and the earlier works. Results were reported in terms of WSS, dimensionless concentration along the lumen/endothelium interface, temperature fields and temperature profiles for external and internal heating at different curvature ratios. It was observed that WSS increases slightly along the lumen/endothelium interface when the curvature ratio increases. Also, in the exterior part, at a fixed curvature ratio, the WSS increases slightly, while it decreases slightly at the interior portion. The dimensionless concentration increases along the lumen/endothelium interface as curvature effect, i.e., and increase in the r/R ratio, increases. The thermal analysis has established that conduction is the dominant mode of heat transfer.

REFERENCES

Ai, L. and Vafai, K. [2006], A coupling model for macromolecule transport in a stenosed arterial wall, *International Journal of Heat and Mass Transfer*, Vol. 49, No. 9, pp. 1568-1591.

Alazmi, B. and Vafai, K. [2001], Analysis of fluid flow and heat transfer interfacial conditions between a porous medium and a fluid layer, *International Journal of Heat and Mass Transfer*, Vol. 44, No. 9, pp 1735-1749.

Amiri, A. and Vafai, K. [1994], Analysis of dispersion effects and non-thermal equilibrium, non-Darcian, variable porosity incompressible flow through porous media, *International Journal of Heat and Mass Transfer*, Vol. 37, No. 6, pp. 939-954.

Chung, S. and Vafai, K. [2012], Effect of the fluid–structure interactions on low-density lipoprotein transport within a multi-layered arterial wall, *Journal of biomechanics*, Vol. 45, No. 2, pp. 371-381.

Chung, S. and Vafai, K. [2013], Low-density lipoprotein transport within a multi-layered arterial wall—Effect of the atherosclerotic plaque/stenosis, *Journal of biomechanics*, Vol. 46, No. 3, pp. 574-585.

Chung, S. and Vafai, K. [2014], Mechanobiology of low-density lipoprotein transport within an arterial wall—impact of hyperthermia and coupling effects, *Journal of biomechanics*, Vol. 47, No. 1, pp. 137-147.

Duck, F. A. [1990], *Physical properties of tissues: a comprehensive reference book*, San Diego Academic Press Inc.

Iasiello, M., Vafai, K., Andreozzi, A., Bianco, N. and Tavakkoli, F. [2015], Effects of external and internal hyperthermia on LDL transport and accumulation within an arterial wall in the presence of a stenosis, *Annals of biomedical engineering*, Vol. 43, No. 7, pp. 1585-1599.

Iasiello, M., Vafai, K., Andreozzi, A. and Bianco, N. [2016a],Low-density lipoprotein transport through an arterial wall under hyperthermia and hypertension conditions–An analytical solution, *Journal of biomechanics*, Vol. 49, No. 2, pp. 193-204.

Iasiello, M., Vafai, K., Andreozzi, A. and Bianco, N. [2016b], Analysis of non-Newtonian effects on Low-Density Lipoprotein accumulation in an artery, *Journal of biomechanics*, Vol. 49, No. 9, pp. 1437-1446.

Karner, G., Perktold, K. and Zehentner, H. P. [2001], Computational modeling of macromolecule transport in the arterial wall. *Computer Methods in Biomechanics and Biomedical Engineering*, *4*(6), 491-504.

Katz, M. A. [1985], New formulation of water and macromolecular flux which corrects for non-ideality: theory and derivation, predictions, and experimental results. *Journal of theoretical biology*, *112*(2), 369-401.

Kenjereš, S. and de Loor, A. [2014], Modelling and simulation of low-density lipoprotein transport through multi-layered wall of an anatomically realistic carotid artery bifurcation, *Journal of The Royal Society Interface*, Vol. 11, No. 91, Article number 20130941.

Khakpour, M. and Vafai, K. [2008], A comprehensive analytical solution of macromolecular transport within an artery, *International Journal of Heat and Mass Transfer*, Vol. 51, No. 11, pp. 2905-2913.

Kolios, M. C., Sherar, M. D. and Hunt, J. W. [1995], Large blood vessel cooling in heated tissues: a numerical study, *Physics in Medicine and Biology*, Vol. 40, No. 4, pp. 477-494.

Köster R, Kähler J, Brockhoff C, Münzel T and Meinertz T [2002], Laser coronary angioplasty: history, present and future, *Am J Cardiovasc Drugs*, Vol. 2, No. 3, pp. 197-207.

Nematollahi, A., Shirani, E., Mirzaee, I. and Sadeghi, M. R. [2012], Numerical simulation of LDL particles mass transport in human carotid artery under steady state conditions, *Scientia Iranica*, Vol. 19, No.3, pp. 519-524.

Olgac, U., Kurtcuoglu, V. and Poulikakos, D. [2008], Computational modeling of coupled blood-wall mass transport of LDL: effects of local wall shear stress, *American Journal of Physiology-Heart and Circulatory Physiology*, Vol. 294, No. 2, H909-H919.

Platten, J. K. [2006], The Soret effect: a review of recent experimental results, *Journal of applied mechanics*, Vol. 73, No. 1, pp. 5-15.

Prosi, M., Zunino, P., Perktold, K. and Quarteroni, A. [2005], Mathematical and numerical models for transfer of low-density lipoproteins through the arterial walls: a new methodology for the model set up with applications to the study of disturbed lumenal flow, *Journal of biomechanics*, Vol. 38, No.4, pp. 903-917.

Stangeby, D. K. and Ethier, C. R. [2002], Computational analysis of coupled blood-wall arterial LDL transport, *Journal of biomechanical engineering*, Vol.124, No. 1, pp.1-8.

Wada, S. and Karino, T. [2000], Computational study on LDL transfer from flowing blood to arterial walls, In *Clinical Application of Computational Mechanics to the Cardiovascular System* (pp. 157-173), Springer Japan.

Wang, S. and Vafai, K. [2015], Analysis of low density lipoprotein (LDL) transport within a curved artery,*Annals of biomedical engineering*, Vol. 43, No. 7, pp. 1571-1584.

Yang, N. and Vafai, K. [2006], Modeling of low-density lipoprotein (LDL) transport in the artery—effects of hypertension, *International Journal of Heat and Mass Transfer*, Vol. 49, No. 5, pp. 850-867.